PHYSICAL REVIEW B VOLUME 55, NUMBER 14 1 APRIL 1997-II

Resonant OH^- photodissociation in alkali halide crystals

L. Gomes* and S. P. Morato
Instituto de Pesquisas Energéticas e Nucleares, Comissão Nacional de Energia Nuclear, Caixa Postal 11049,
Pinheiros, 05422-970, Brazil

(Received 11 September 1996)

The comprehensive study of resonant OH^- photodissociation in several alkali halides hosts showed that deep traps for electrons can be produced from the OH^- dissociation. These traps can be effective for the capture of electrons produced from the radiation damage of the lattice as well as for trapping electrons from ionized color centers. A new photodissociation channel of OH^- defects was observed for the deexcitation of the $(OH^-)^*$ (* represents the excited state) molecule in KI and RbI hosts. This effect can be effective only when the lattice around the molecule holds a large enough interstitial space. This new mechanism is responsible for the strong production, at 77 K, of F centers and OH^0 molecules at the expenses of OH^- defects. Considering the complete investigation of the full cycle (photodissociation→thermal and optical treatments→back production of OH^- defects) a phenomenological model was proposed that would explain the observed behavior when one covers a wide variation of lattice parameters (KCl→RbI). Looking into the energy level diagram of OH^- and F centers in alkali halides as a function of lattice parameter, one observes that, for KI and RbI, the unrelaxed ground state of the F center energetically overlaps with the relaxed excited state of the OH^- ion. [S0163-1829(97)01113-2]

I. INTRODUCTION

The study of basic properties of extrinsic molecular impurities in solids, as well as their interaction with intrinsic defects produced by the radiation damage in the host lattice,[1–6] has given valuable contributions for the development of lasers emitting in the near and middle infrared region of the spectra. In particular, F centers in alkali halides have their optical properties drastically modified by the presence of OH^- defects in the lattice.[7] In the aggregate case, a new defect can be produced: the $F_H(OH^-)$ center.[7] OH^- impurities can also be used to stabilize F_2^+ centers after high-energy irradiation with electrons or gamma rays.[8–11] Recently, a new complex defect has been observed in the OH^- doped LiF crystal after gamma irradiation at −20 °C, due to a water molecule capture by an F_Z center.[12]

The presence of OH^- impurities in the alkali host enriches the physical properties of the crystal because they can be photodissociated by UV irradiation resonantly with its electronic transition.[13,14] The primary products of such photodissociation are known to be the interstitial neutral hydrogen atom, $H_1{}^0$ (U_2 center) and the substitutional negative oxygen ion, $O_S{}^-$ centers.[15] In this case, the radiation damage is done at low energies (6 eV) involving a very simple mechanism of primary defect production and constitutes an important tool to investigate all the secondary products, following the OH^- dissociation, due to temperature effects.

The OH^- impurity can be found in substitutional sites[16–18] or associated with Me^{2+} impurities (where Me^{2+} stands for alkaline and transition-metal ions) in several laser crystals synthetically grown.[19,20] Since it has a large electric dipole moment it can work many times as a sink center absorbing the migrating excitation energy from activators emitting in the 2.7–3.0 μm region.[21,22] This survey of effects has stimulated the investigation of the OH^- optical properties in both ground and excited states.[23,24] However, their behavior under UV resonant electronic excitation has not yet been completely understood. The lattice parameter and temperature can affect the excited-state dynamic of this molecular ion because their electronic transition involves a charge transfer with the cationic (A^+) neighborhood. (A^+) stands for alkali-metal ions.

The electronic ground state of the OH^- defect is described by a $\{OH^-[X^1\Sigma^+(1\sigma^2 2\sigma^2 3\sigma^2 1\pi^4)]+4S^0(A^+)\}$ configuration, while the excited-state configuration is $\{OH^0[X^2\Pi_i(1\sigma^2 2\sigma^2 3\sigma^2 1\pi^3)]+4S^1(A^0)\}$. The optical excitation of the UV band of the OH^- defect produces two physically distinct effects: a luminescence[25] in the near UV ($300<\lambda<400$ nm) and a photodissociation into a U_2 center and an $O_S{}^-$ center for excitation at low temperatures ($T<100$ K). This proposition is well supported by ESR results[15] which indicated that after the OH^- photodissociation, the hydrogen atoms become interstitial in the lattice. The negative oxygen ion is not well identified by optical absorption because their optical transition is positioned close to the exciton fundamental absorption band in most of the alkali-halide hosts. In this work, we observed this band and followed their thermal extinction. For this purpose, the crystals had to be irradiated with resonant UV(OH^-) light at low temperatures (∼50 K) with exposures no longer than 15 h to avoid the formation of other undesirable centers like substitutional H^- ions (U centers) and F centers.[26,27] By heating the sample, U_2 centers can be thermally activated at $T\geqslant100$ K,[28–30] producing a recombination process not fully efficient (∼20%), partially restoring the photodissociated OH^- ions at the expenses of the O_S^- centers. This process gives rise to a thermally activated luminescence. The U_2 centers can also be converted into an interstitial configuration as U_{2X} centers which are thermally stable up to 150 K. Above this temperature they are destroyed resulting in H_2O^- centers.[29] Finally the H_2O^- centers can be thermally destroyed at temperatures

© 1997 The American Physical Society

TABLE I. A list of the peak positions of the absorption bands of the primary defects products of the OH$^-$ photodissociation after UV irradiation at 77 K in several alkali-halide crystals, observed in this work. All the peak positions are in nanometers. NO represents not observed, s stands for substitutional position in the lattice, i stands for interstitial position, all the absorption bands were measured at 77 K, □ or the α band is due to the electronic transition of an anionic vacancy, the β band is due to the exciton transition nearby an F center, the OH$_i^-$ band is the electronic transition of an OH$^-$ ion located in an interstitial position, produced in KI and RbI.

Host	OH$_S^-$	O$_S^-$	□(α)	H$_i^0$(U_2)	β	OH$_i^-$
KBr	216	196	202	270	192	NO
RbCl	212	192	-	242	-	NO
RbBr	226	NO	206	280	197	360
KI	230	NO	238	339	-	303
						312
RbI	230	NO	-	343	-	349
KBr$^+$ 2% F^-	216	196	202	270	192	333
RbBr$^+$ 1.5% Na$^+$	226	NO	206	280	197	360

above 220 K producing back F centers and H$_2$O interstitial molecules (not yet identified).

All these processes were, so far, not correlated in order to give a complete physical picture of the primary products of OH$^-$ photodissociation. The same can be said regarding the intermediate steps that leave to the final secondary products. The purpose of this paper is to review this subject and clarify the intermediate mechanisms involved for different host lattices.

II. EXPERIMENT

The alkali-halide crystals were grown in our laboratories from ultrapure salts doped with 10^{-5} mol fractions of OH$^-$ impurity and were also obtained from the Crystal Growth Laboratory of the University of Utah. Samples were cleaved in the (100) plane with thickness between 0.7 and 1.0 mm. All the measurements were performed with the samples held in the cold finger of an LNT cryostat chamber from Janis. The pulse annealing experiments were performed due to the use of an exchange gas chamber between the cold finger and the liquid coolant bath. Measurements made at 10–12 K were done using a He-gas closed-cycle refrigerator cryostat from APD Cryogenics. The UV irradiation was done using a 150-W Xe lamp plus a monochromator of 25-cm focal length. High-intensity UV irradiation was done using a 1000-W Xe lamp with interference filters. The absorption spectra were measured using a Cary 17 D (linear in nm) and a Carl Zeiss DMR-21 (linear in cm^{-1}) spectrophotometer. Luminescence measurements were done using two monochromators displayed at 90° to minimize the scattering excitation light into the detector. Excitation was done using a 300-W Xe lamp from Cermax. The detector used was a photomultiplier tube with an S-20 extended cathode from EMI. The luminescence signals were treated with a lock-in amplifier from PAR. IR absorption was measured using a PE 180 spectrophotometer.

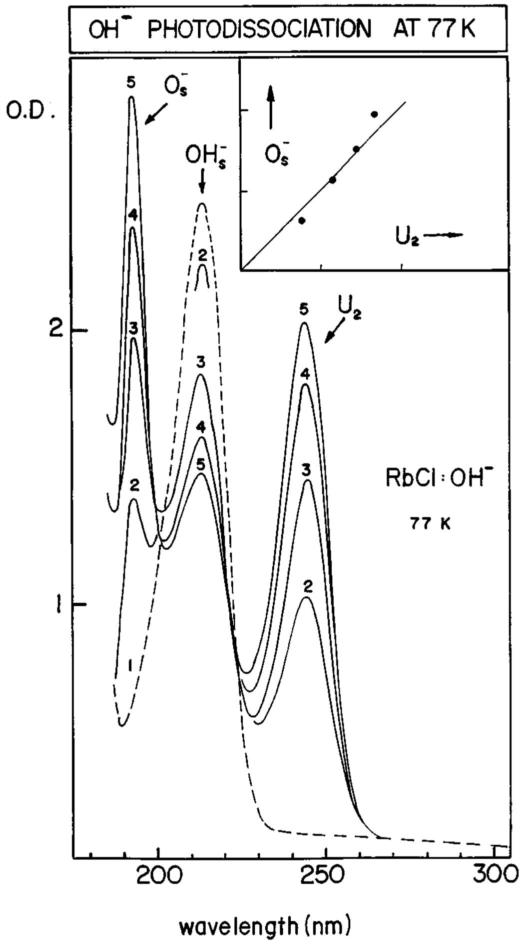

FIG. 1. OH$^-$ photodissociation in RbCl:OH$^-$ at 77 K done with UV (213-nm) irradiation with a Xe lamp of 150 W. (1) Before UV irradiation; (2) after 5 h of UV irradiation; (3) after 11 h; (4) after 16 h; and (5) after a total of 21 h of UV irradiation. The inset shows a linear correlation between the increase of the O$_S^-$ band at 192 nm and the increase of the U_2 band at 242 nm.

III. RESULTS AND DISCUSSION

Until now it was known that the substitutional OH$^-$ ion in alkali halides could be dissociated during a prolonged UV irradiation resonant with the OH$^-$ absorption band at temperatures below 150 K. U_2 centers and O$_S^-$ centers can be observed by UV absorption measurements at LNT in the cases where the photodissociation was done at $T<110$ K. The absorption band maxima of the primary OH$^-$ photodissociation defects found after UV irradiation at 77 K are listed in Table I for several alkali-halide crystals.

A. OH$^-$ photodissociation in RbCl and KBr

Figure 1 shows the results of the OH$^-$ photodissociation in RbCl:OH$^-$ after the UV irradiation at 212 nm at 77 K. Initially the crystal shows the OH$^-$ band at 212 nm. Increasing the UV irradiation time, the U_2 centers absorbing at 242 nm and the O$_S^-$ band at 192 nm grow up at the expense of OH$_S^-$ defects. A linear correlation is seen between both band growths (see the inset in Fig. 1). Figure 2 shows a similar result for the KBr:OH$^-$ crystal. In this case, the U_2 band peaks at 270 nm and the O$_S^-$ band peaks at 196 nm.

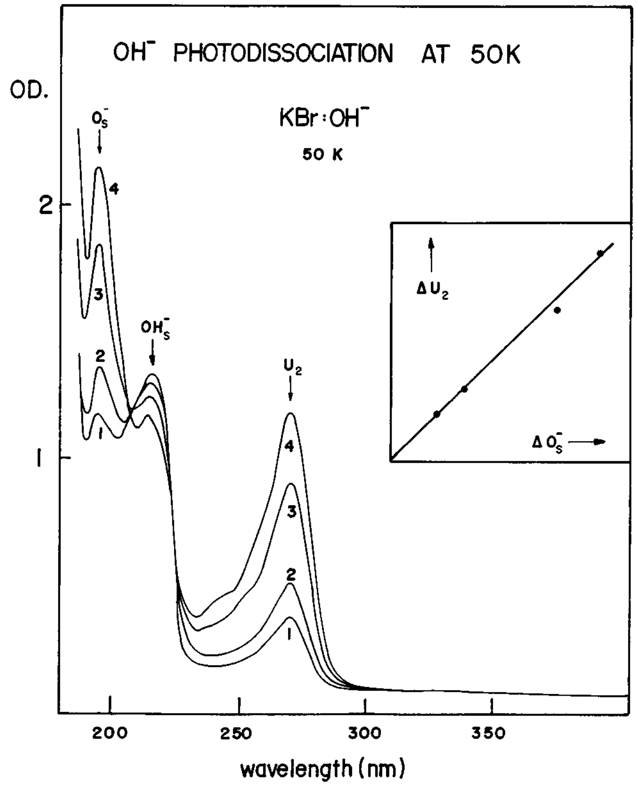

FIG. 2. OH$^-$ photodissociation in KBr:OH at 50 K done with UV (214 nm) irradiation with a Xe lamp of 150 W. (1) After 17 h of UV irradiation; (2) after 21 h irradiation; (3) after 38 h; and (4) after a total of 54 h of UV irradiation at 50 K. The inset shows a linear correlation between the increase of the O_S^- band at 196 nm and the increase of the U_2 band at 270 nm.

These results totally agree with what is commonly found in the literature for the OH$^-$ photodissociation. The presence of U_2 centers is well established by electron-nuclear double-resonance (ENDOR) experiments in KCl.[15] On the other hand, the structural configuration of the negative oxygen ion produced in the OH$^-$ photodissociation is not well established until now. It is found by the ENDOR experiments that this ion is located in the substitutional position in RbCl.[31]

In order to better investigate the O_S^- band we submitted the KBr crystal with the OH_S^- defects previously photodissociated, to an intense UV irradiation with $\lambda<200$ nm at 50 K, using a 1000-W Xe lamp and an interference filter. The results are presented in Fig. 3. It shows a destruction of the O_S^- band at 196 nm and the formation of α (□) centers absorbing at 202 nm. The increase in the absorption at $\lambda<191$ nm is due to the presence of O$^-$ interstitial ions which absorb near the exciton fundamental bands. The inset in Fig. 3 clearly shows a linear correlation between the α center formation with the presence of O$^-$ interstitial oxygen centers. A partial conclusion is that an O_S^- center, when excited into their respective absorption at 196 nm, can be destroyed producing an anionic vacancy (α centers) and an interstitial negative oxygen ion (O_i^- centers). The O_i^- absorption band cannot be resolved due to its superposition with the exciton absorption band in KBr. The thermal destruction of α centers in KBr was performed well after the optical bleaching of F centers that were originally produced after the H_2O^- center's thermal destruction at 220 K.

The H_2O^- center is one of the secondary products of OH$^-$ defects. It is produced by the reaction between the mobile hydrogen atoms and the OH$^-$ impurities. Figure 4 shows the results of the α center's thermal bleaching induced by several thermal pulses from 231 to 350 K. With the increase in temperature, in the range from 230 to 260 K, the anionic vacancy randomly moves through the lattice. During this diffusion it may be captured by an interstitial negative oxygen ion producing an intermediate configuration between the O_i^- and the O_S^- defects. We called this configuration an O_i^- (□) center which is stable up to 260 K. It produces an absorption band at 199 nm. In this configuration, the perturbation in the O_i^- center transition caused by the nearby anionic

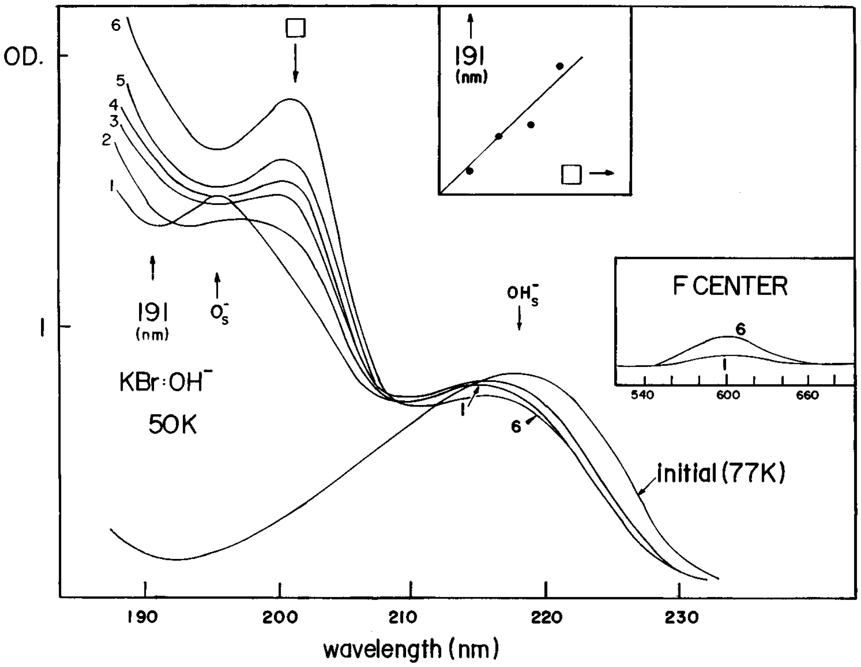

FIG. 3. Optical bleaching of the O_S^- centers in KBr:OH$^-$ at 50 K. The optical bleaching was done using an intense UV irradiation with a 1000-W Xe lamp+an interference filter at 200 nm. (1) initial spectrum obtained well after the OH$^-$ photodissociation at 50 K done using a 150-W Xe lamp; (2) after 15 sec of intense UV irradiation; (3) after 55 sec; (4) after 1 min and 45 sec; (5) after 2 min and 45 sec; (6) after a total of 5 min of intense UV irradiation. One of the insets shows the linear correlation obtained between the absorption intensity at 191 nm and the absorption peak of α centers at 202 nm. Also, the participation of F centers in this process is negligible as is shown by one of the insets.

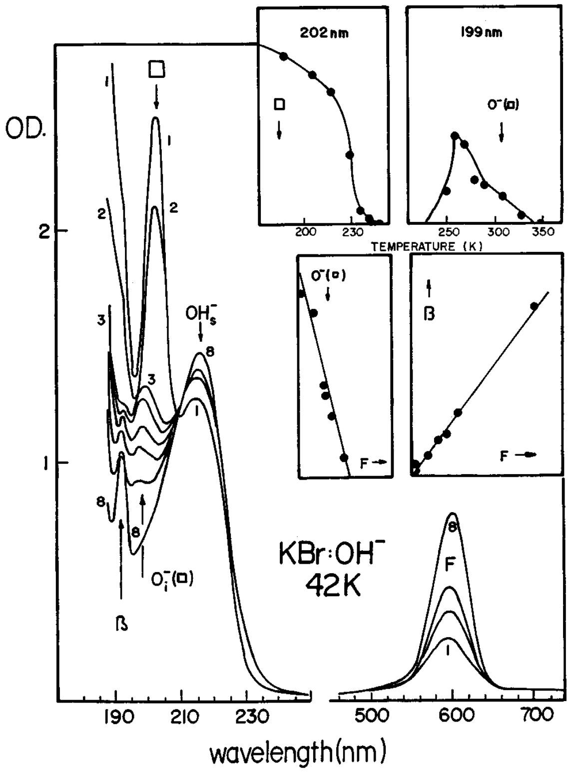

FIG. 4. Thermal bleaching of α centers induced by a pulsed thermal annealing in KBr:OH$^-$. (1) Initial spectrum measured at 42 K showing mainly the α band at 202 nm produced after intense UV (OH$^-$) irradiation; (2) after a pulse of 231 K; (3) after a pulse of $T=260$ K; (4) after $T=270$ K; (5) after $T=280$ K; (6) after $T=310$ K; (7) after $T=329$ K; and (8) after $T=350$ K. Two insets (upper) show the temperature effect on the α band and also for the absorption at 199 nm which is attributed to O_i^-(□) centers. Two insets show the linear correlations (a) between the change in the O_i^-(□) band at 199 nm and the change in the F center absorption band; (b) between the change in the β band at 192 nm and the change in the F band.

vacancy displaces the absorption peak towards ~199 nm. This transition can be regarded as an electronic charge exchange between the negative oxygen ion and the vacancy. This band indicated the existence of an intermediate configuration before a 56% recovery of the initially bleached F centers. In the final destruction of O_i^- (□) centers at 260 K, the electron is transferred to the vacancy forming an F center and leaving an atomic neutral oxygen which can be stabilized as an O_i^0 defect. The following reactions illustrate the observed mechanisms.

(1) OH_S^- photodissociation:

$$OH_s^- + h\nu(OH^-) \text{—} 50\ \text{K} \rightarrow O_s^- + H_i^0(U_2).$$

(2) O^- photodestruction:

$$O_s^- + h\nu(O^-)(\text{at } 50\ \text{K}) \text{—} \sim 100\% \rightarrow \square(\alpha) + O_i^- .$$

(3) H_2O^- thermal destruction:

$$H_2O^- + KT\ \ (300\ \text{K}) \text{—} 100\% \rightarrow F\ \ \text{centers} + O_i^0 + (H_2)_i .$$

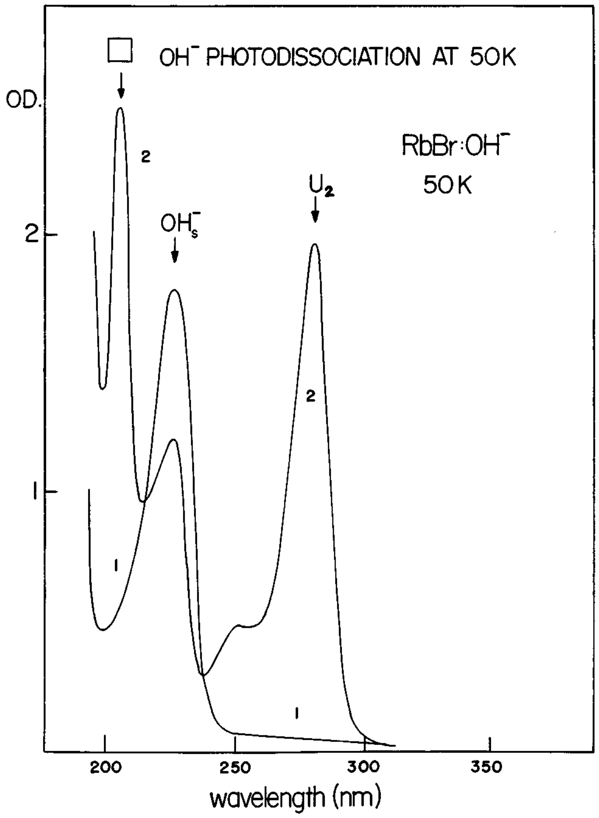

FIG. 5. OH$^-$ photodissociation in RbBr (at 50 K) by an UV (226 nm) irradiation using a 150-W Xe lamp. (1) Initial spectrum measured at 50 K; (2) after 17 h of UV irradiation.

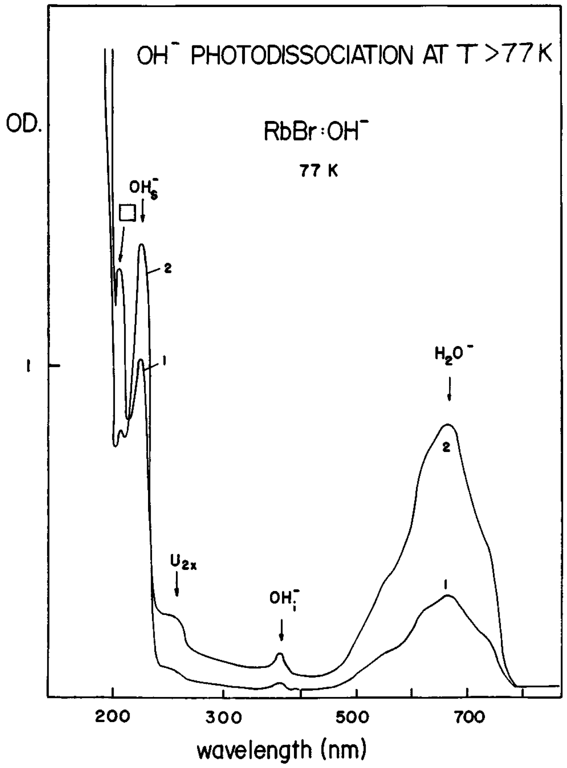

FIG. 6. OH$^-$ photodissociation in RbBr at 120 and 150 K. (1) Spectrum measured at 77 K after 2 h of UV (226 nm) irradiation at 120 K using a 150-W Xe lamp; (2) after 2 h more of UV (226 nm) irradiation at 150 K. H_2O^- and OH_i^- defects are mainly formed.

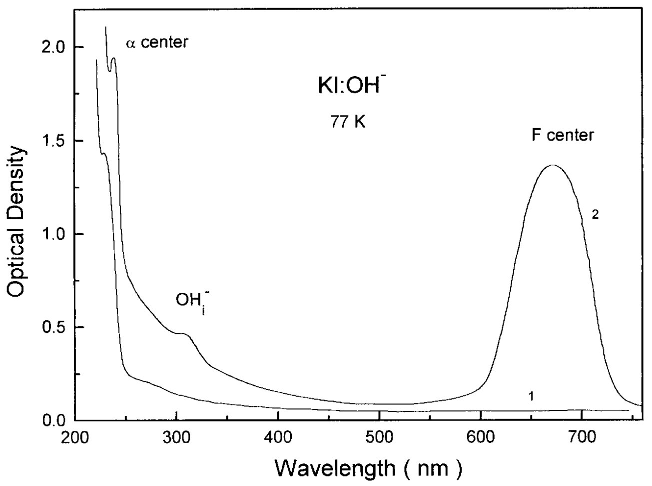

FIG. 7. OH$^-$ photodissociation in KI at 77 K produced by an UV (230 nm) irradiation using a 150-W Xe lamp. (1) Initial spectrum measured at 77 K; (2) after 15 h of UV (230 nm) irradiation at 77 K. *F* centers are directly produced. A new band at 312 nm is seen.

(4) *F* centers optical bleaching:

$$F\ \text{centers}+\text{O}_i^{\,0}+h\nu(F)\ \ (\text{at } 77\ \text{K})\text{—}64\%\text{→}\Box(\alpha)+\text{O}_i^{\,-}.$$

(5) α centers thermal destruction:

$$\Box(\alpha)+\text{O}_i^{\,-}+KT(260\ \text{K})\rightarrow\text{O}_i^{\,-}(\Box),$$

$$\text{O}_i^{\,-}(\Box)+KT(>260\ \text{K})\text{—}56\%\text{→}F\ \ \text{centers}+\text{O}_i^{\,0}.$$

B. OH$^-$ photodissociation in RbBr

The OH$^-$ photodissociation in RbBr crystals with monochromatic light at 236 nm at 50 K produces directly α centers and U_2 centers as primary products. Figure 5 shows this result exhibiting the α band at 206 nm and the U_2 band at 280 nm. As U_2 centers become unstable at temperatures above 110 K, we also explored the OH$^-$ photodissociation at 120 and 150 K. Figure 6 shows the observed results in this case. H$_2$O$^-$ defects are created as a consequence of the U_2 and U_{2X} thermal destruction. A new band at 360 nm was produced in this case, due to the production of OH$^-$ molecule ions in the interstitial positions (see the next section for more details about the OH$^-$ photodissociation in KI and RbI). Comparing the lattice parameter of RbBr (a_i=2.69 Å) with the one of KBr (a_i=2.54 Å) one must conclude that the available interstitial space for RbBr is larger than for KBr. As a consequence, the negative oxygen ion produced in the OH$^-$ photodissociation can leave the vacancy and be stabilized in an interstitial position as an O$_i^-$ defect. The following reaction takes place:

$$\text{OH}_s^{\,-}+h\nu(\text{OH}^-)\ \ (50\ \ \text{K})\text{—}\sim 100\%\text{→}\Box(\alpha)+\text{O}_i^{\,-}+\text{H}_i^{\,0}(U_2).$$

C. OH$^-$ photodissociation in KI and RbI

The OH$^-$ photodissociation in KI and RbI hosts showed very surprising results. Instead of the thermal creation of U_2 and O$_S^-$ or O$_i^-$ centers, pronounced *F* and α center formations were observed as primary products of the OH$^-$ photodissociation at 77 K. Figures 7 and 8 show these results. Besides the *F* and α bands, new absorption bands at 303 and 312 nm for KI and at 349 nm for RbI were seen. These bands are due to the OH$^-$ interstitial ions produced as a result of the F^* ($2p$ excited state of *F* center) electron capture by the OH^0 interstitial molecule directly produced by the OH$^-$ photodissociation. This assumption is supported by the observa-

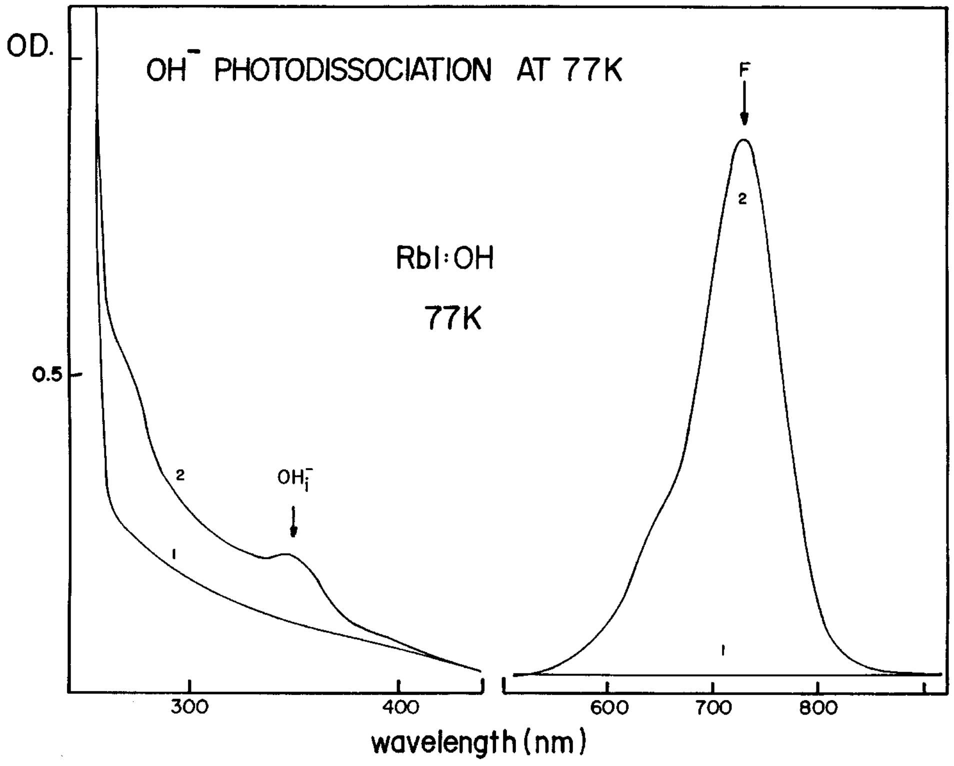

FIG. 8. OH$^-$ photodissociation in RbI at 77 K produced by an UV (230 nm) irradiation using a 150-W Xe lamp. (1) Initial spectrum measured at 77 K; (2) after 20 h of UV (230 nm) irradiation at 77 K. *F* centers are directly produced. A new band at 349 nm is produced.

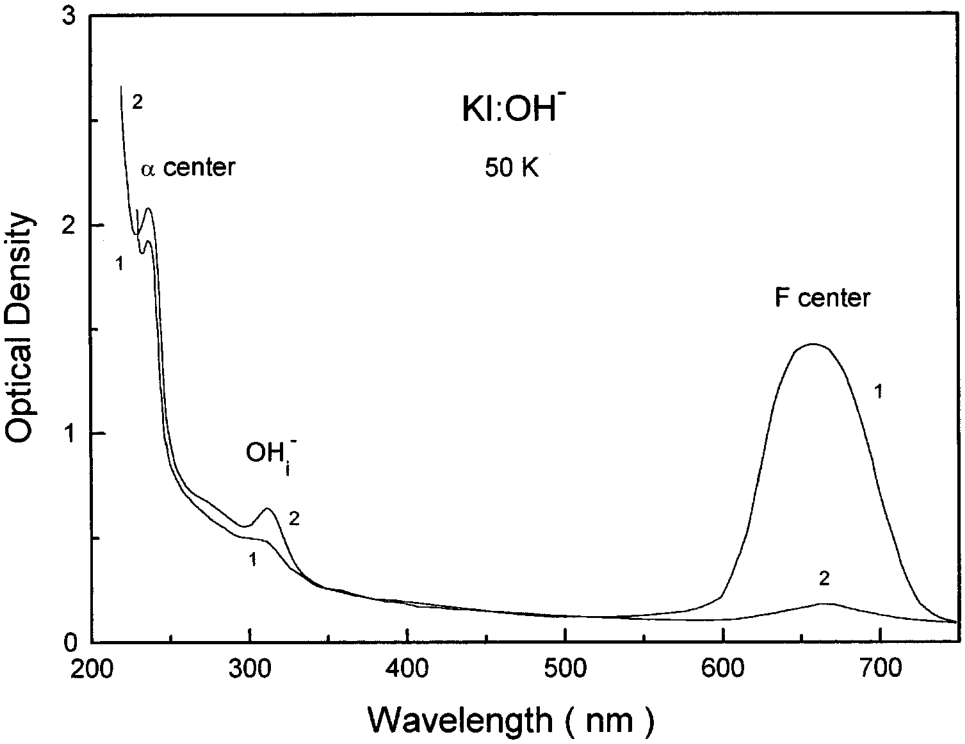

FIG. 9. Optical bleaching of the F centers primary produced by the OH^- photodissociation in $KI:OH^-$ at 77 K. (1) Spectrum measured at 50 K after OH^- photodissociation (17 h of UV irradiation at 77 K); (2) after 21 h of visible irradiation (at 50 K) using a 150-W Xe lamp+KG-4 filter +standard glass filter of 6 mm of thickness.

tion of the optical bleaching of the F centers produced directly by the OH^- photodissociation. Figure 9 shows the results of the F centers bleaching for the photodissociated $KI:OH^-$ at 50 K. There, it is seen that the absorption band at 312 nm is strongly increased at the expenses of the destroyed F centers. Below 50 K, there are no vacancies or ion (or atoms) migrations which can justify this band formation with any involvement with hydrogen and oxygen centers. The bleaching of F centers at 50 K clearly indicates that the F^* $(2p)$ electron tunnels to a trap ion produced direct from the OH^- photodissociation. This trap ion must have a high electron affinity and cannot be either hydrogen or oxygen neutral atoms because H^- and O^- interstitial centers whose absorption bands are very well known are not observed in this process.

Infrared absorption measurements in OH^- photodissociated KI and RbI (at 77 K) exhibited a new absorption near the OH^- stretching band. Figure 10(a) shows the obtained results for the OH^- photodissociation in $KI:OH^-$ at 77 K. The initial OH^- stretching absorption band at 2774.5 nm was reduced to ~34% of its initial intensity in this irradiation process and a new band at 2765 nm was produced. Figures 10(b) and 11 show the temperature effects on the new absorption bands at 2765 nm for KI and 2769 nm for RbI. It was verified that these new IR absorptions localized at the high-energy side of the very known OH^- stretching absorption band were produced only in the $UV(OH^-)$ irradiation at $T>50$ K, i.e., in the temperature range where the F centers are directly formed at the expenses of the excited OH^- defects. These results also reinforce our previous statement that interstitial OH^0 molecules and OH^- ions are produced due to the OH^- center's ionization in KI and RbI crystals. The interstitial OH^0 molecule does not exhibit an electronic absorption band in the investigated spectral range. On the other hand, the OH^- photodissociation in these two hosts, at lower temperatures ($T\leqslant 50$ K), produces the normal primary products as U_2 and α centers. Figure 12 shows the result of the OH^- photodissociation in KI at 50 K and the temperature effects on the stability of the primary centers. There it is seen, for example, that U_2 centers are unstable at 77 K and U_{2X} centers are unstable above 150 K. H_2O^- centers are formed by the U_2 and U_{2X} destruction. The thermal destruction of H_2O^- centers at 260 K, produces F and OH_i^- (new band) centers. The following reactions are proposed for these two hosts.

---

(1) OH photodissociation:

$$OH_s^- + h\nu(OH^-) \rightarrow (50\ \text{K}) \text{—} \sim 100\% \rightarrow \square(\alpha) + O_i^- + H_i^0(U_2),$$

$$(77\ \text{K}) \text{—} \sim 100\% \rightarrow F\ \text{centers} + (OH^0)_i .$$

(2) F centers optical bleaching:

$$F\ \text{centers} + (OH^0)_i + h\nu(F)(50\ \text{K}) \rightarrow \text{—} \sim 100\% \rightarrow \square(\alpha) + (OH^-)_i \quad \text{(new band at 312 nm)}.$$

(3) H_2O^-thermal destruction:

$$H_2O^- + KT(300\ \text{K}) \text{—} \sim 100\% \rightarrow F\ \text{centers} + (OH^0)_i + 1/2H_2 .$$

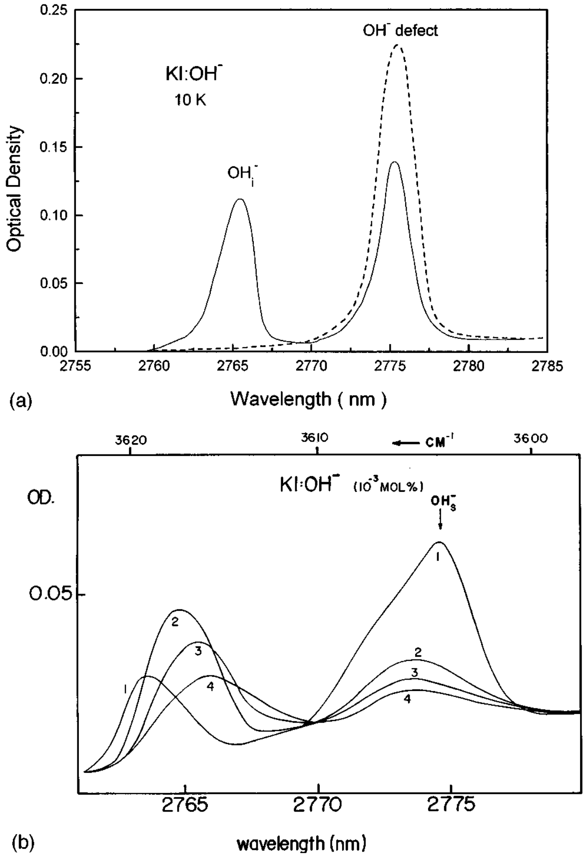

FIG. 10. (a) Infrared spectrum of KI:OH$^-$ before (dashed line) and after a partial (30%) OH$^-$ photodissociation (solid line) by 15 h of UV (230 nm) irradiation at 77 K with a 150-W Xe lamp. The new absorption peak at 2765 nm is attributed to the interstitial OH$^-$ ions. (b) Infrared spectrum of OH$^-$ photodissociated KI:OH$^-$ after 15 h of UV (230 nm) irradiation at 77 K. The temperature effect is shown on the new absorption bands at 2765 nm in comparison with the fundamental absorption of OH$^-$ defects at 2774.5 nm. (1) Spectrum measured at 10 K; (2) at 50 K; (3) at 90 K; and (4) at 130 K.

D. Mixture of both channels of OH$^-$ photodissociation in Na$^+$-doped RbBr and F$^-$-doped KBr hosts

The new channel of OH$^-$ photodissociation which has been observed in KI and RbI can be activated in KBr and RbBr by doping these crystals with F$^-$ (2%) and Na$^+$ (1.5%), respectively. In the case of KBr: F$^-$(2%):OH$^-$ it is very clearly seen the mixture of primary products from both channels of OH$^-$ photodissociation done with monochromatic light at 216 nm at 77 K (Fig. 13). By increasing the irradiation time, U_2 centers, α and F centers are formed at the expenses of OH$^-$ defects. The formation of the new band is seen at 333 nm due to the OH$^-$ interstitial molecular ions. The OH$^-$ photodissociation in RbBr:Na$^+$(1.5%):OH$^-$ at 77 K also exhibits the mixture of defects produced from both channels of OH$^-$ photodissociation (see Fig. 14). In this case, the OH$_i^-$ band at 360 nm were very pronounced. In both cases, after investigating the thermal stability of H$_2$O$^-$ centers, we concluded that the F center formation process observed in the OH$^-$ photodissociation at 77 K cannot be attributed to the thermal instability of H$_2$O$^-$ centers, which is found to be stable up to 180 K. The smaller ionic size of Na$^+$ and F$^-$ compared with the Rb$^+$ and Br$^-$ lattice ions propitiate available interstitial space in the respective hosts, to accommodate the OH^0 molecule nearby those impurities (Na$^+$ and F$^-$). As a consequence, this new channel of OH$^-$ photodissociation could compete with the dissociative one.

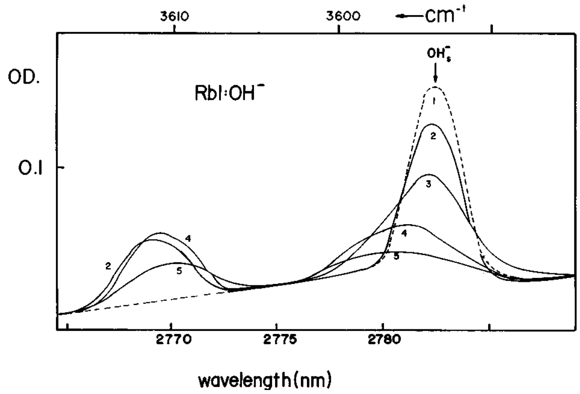

FIG. 11. Infrared spectrum of OH$^-$ photodissociated RbI:OH$^-$ after 32 h of UV (230 nm) irradiation at 77 K. The temperature effect is shown on the new absorption bands at 2769 nm in comparison with the fundamental absorption of OH$^-$ defects at 2782.5 nm. (1) Spectrum measured at 10 K before UV irradiation; (2) spectrum measured at 10 K after UV irradiation; (3) at 30 K; (4) at 50 K, and (5) at 90 K. (2)–(5) were also measured after the UV irradiation.

E. OH$^-$ fluorescence in KI

The fluorescence spectra of OH$^-$ defects measured at 8 K are presented in Fig. 15 for KBr, RbBr, and KI crystals containing 1×10^{17} OH$^-$/cm^3. The most intense fluorescence peak is due to the electronic transition from the [OH^0($1\sigma^2 2\sigma^2 3\sigma^2 1\pi^3$): $4S^1(K^0)$] excited state to the [OH$^-$($1\sigma^2 2\sigma^2 3\sigma^2 1\pi^4$): $4S^0(K^+)$] ground state of the OH$^-$ defect without the vibrational stretching excitation

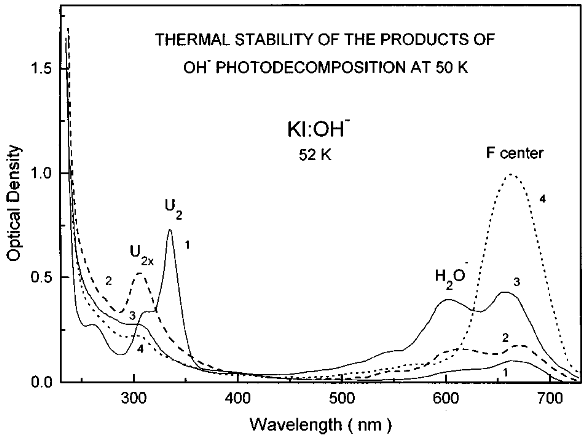

FIG. 12. Thermal stability of the primary defects produced by the OH$^-$ photodissociation in KI at 50 K. Absorption measurements were done at 50 K (1) after the UV (230 nm) irradiation by 15 h; (2) after a pulse of temperature of $T=67$ K; (3) after $T=177$ K; and (4) after $T=260$ K. U_2 and U_{2x} centers are thermally unstable at 77 K and above 150 K, respectively, in KI H$_2$O$^-$ defects are formed at the expenses of U_2 and U_{2x} destruction. F centers are formed by the H$_2$O$^-$ defect destruction at 260 K.

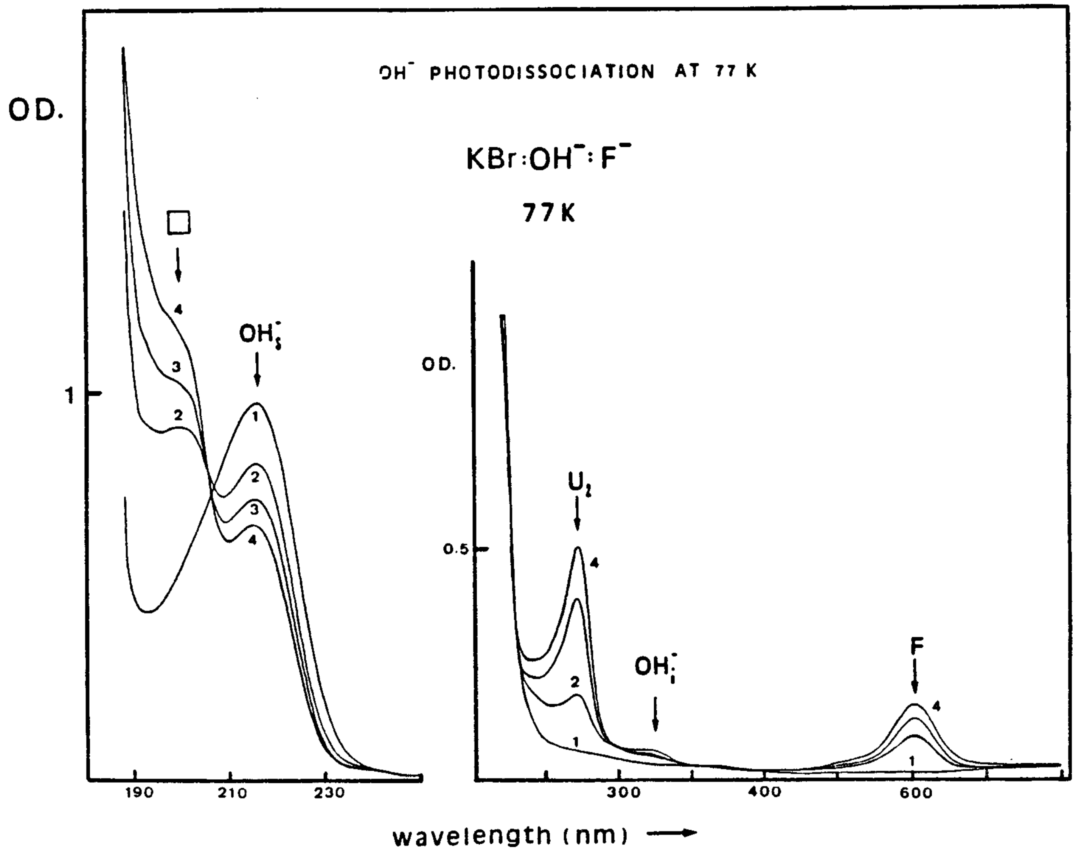

FIG. 13. OH$^-$ photodissociation in KBr:F$^-$ (2%):OH$^-$ at 77 K. The absorption spectra were measured at 77 K. (1) Spectrum measured before the UV (OH) irradiation. There only the UV (OH$^-$) absorption is seen (2) after 15 h of UV (216 nm) irradiation at 77 K using a 150-W Xe lamp+interference filter; (3) after one more hour of UV (216 nm) irradiation using a 1000-W Xe lamp+interference filter; and (4) after two more hours (idem 3). The new channel of OH$^-$ photodissociation which produces *F* centers now competes with the U_2 center formation in this fluorine-doped KBr host.

($n'=0\rightarrow n=0$, where n' and n denote the quantum vibrational number for the excited and ground states of the vibrational oscillator, respectively). The other two peaks are due to the electronic transition involving one ($n'=0\rightarrow n=1$) and two ($n'=0\rightarrow n=2$) stretching mode excitations. The energy separation between the closest peaks corresponds to the stretching vibrational mode energy of the OH$^-$ molecule in the substitutional position. On the right side of Fig. 15 one finds the excitation bands of these fluorescence which are coincident with the absorption peaks of OH$_S^-$ defects. As the lattice parameter of the hosts increases, the excitation and fluorescence peaks shift to lower energies.

In the following cases, all these samples were irradiated with UV (OH$^-$) monochromatic light for 19 h at 10 K using a Xe lamp of 150 W. Figure 16 shows the fluorescence spectra of OH$^-$ measured at 8 K well after the UV irradiation. For KBr and RbBr hosts, no trace of remaining OH$^-$ defects was seen. Instead of that, a new broad band at 490 nm in KBr, at 510 nm in RbBr, and 540 nm in KI have appeared. Looking at their excitation peaks we attributed these emission bands as due to α centers, which are produced during the OH$^-$ photodissociation. On the top of the emission band of α centers in KI, a fine structure is observed due to the narrow emission lines of O$_2^-$ centers which absorb also near 240 nm. These molecular defects are formed in very low amounts ($\sim 1\times 10^{16}$ cm^{-3}) during the OH$^-$ photodissociation.

An important fact is obtained when a correlation is made between the thermal effects on the new absorption band at 312 nm (attributed to the OH$_i^-$ ions) presented in Fig. 17 (curve 1→2 after $T=240$ K) with the thermal effects also verified in the emission spectrum of OH$^-$ photodissociated KI exhibited in Fig. 16 (curve 1→2 after $T=240$ K). The new emission band at 361 nm observed in KI:OH$^-$ after the OH$^-$ photodissociation [Fig. 16 (curve 1)] may be due to OH$^-$ interstitial ions produced together with α centers by the second dissociation channel of OH$^-$ defects. It is known by this work that a new channel of OH$^-$ photodissociation is effective in KI at 77 K which produces *F* centers and interstitial OH^0 molecules. These molecules can capture *F* electrons forming interstitial OH$^-$ molecules responsible for the appearance of the 312-nm band. As a consequence, α centers are formed too. Figure 17 shows that the absorption band at 312 nm shifts to 303 nm after a thermal pulse of 240 K in KI while the α absorption band at 238 nm shifts its position to 231 nm. It means that the 303-nm band is due to the OH$_i^-$ ions perturbed by the α centers, and that this perturbation effect also extends to the α band which shifts its maximum towards the OH$_S^-$ original position. As the peak temperature of the pulse annealing increases to 300 K, both the 303-nm band and the perturbed α band disappear, restoring the original OH$_S^-$ band at 230 nm (curve 4 of Fig. 17). Figure 16 shows the correspondence of the emission bands of KI after a partial OH$^-$ photodissociation, exhibiting the same tem-

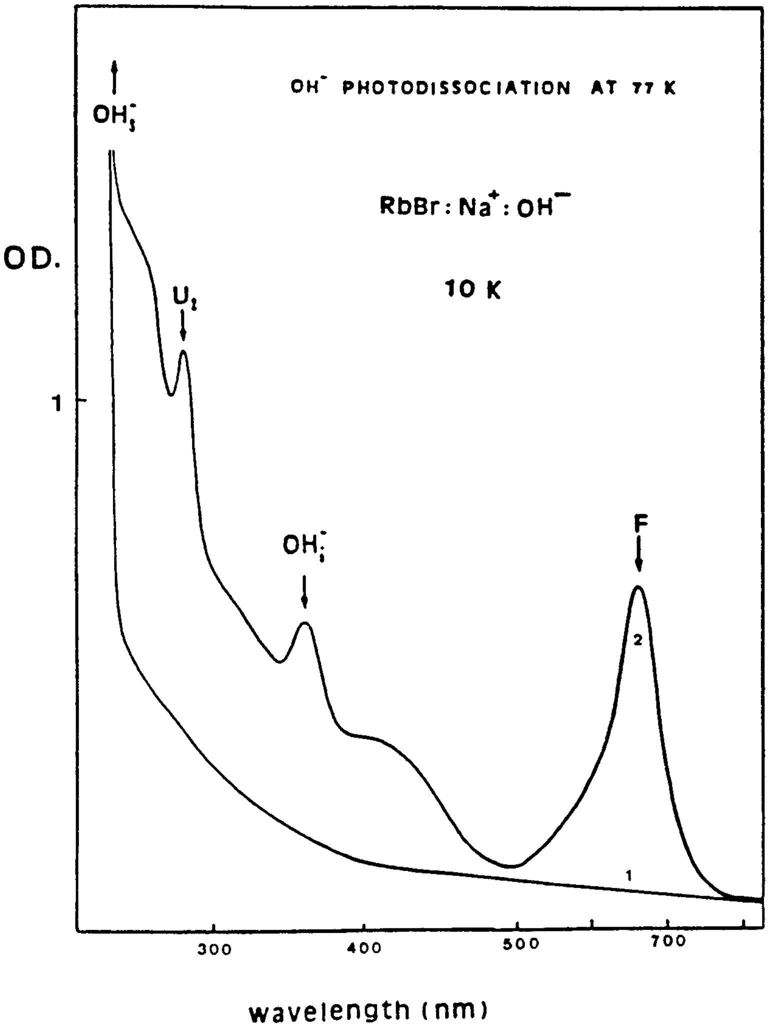

FIG. 14. OH$^-$ photodissociation in RbBr:Na$^+$ (1.5%):OH$^-$ at 77 K. The absorption spectra were measured at 10 K. (1) Spectrum measured before the UV (OH$^-$) irradiation, (2) after 17 h of UV (226 nm) irradiation at 77 K using a 150-W Xe lamp+an interference filter. *F* centers and the new absorption band at 360 nm are seen.

perature effects. Curve 1 of Fig. 16 was obtained well after the OH$^-$ photodissociation and exhibits, besides the α band, a modified emission band around the OH$^-$ fluorescence. This modified band can be due to the OH$^-$ interstitial ions which are formed by the second channel of photodissociation. By increasing the temperature up to 240 K, the α centers are partially destroyed as are shown by curve 2 of Figs. 16 and 17. In both absorption (Fig. 17) and emission (Fig. 16) spectra, a decrease is seen of α and (312–303) nm bands and the restoration of the OH$_S^-$ defects previously dissociated.

IV. PROPOSED MODEL FOR THE NEW CHANNEL OF OH$^-$ PHOTODISSOCIATION

Considering that *F* centers are produced as primary defects from the OH$^-$ photodissociation in some hosts as KI and RbI at 77 K, we will try to make an empirical correlation between the total energies of ground and excited states of both defects involved, *F* and OH$^-$. For that purpose, the energy positions were calculated of ground and excited states of OH$_S^-$ (relaxed and unrelaxed states) assuming that the dissipated energy in both states is equal and that the total dissipated energy should be the energy difference between the energy of the UV(OH$^-$) absorption band and the energy of the OH$^-$ emission band. Also, considering that the electronic transition of OH$_S^-$ involves a charge transfer to the neighboring cation (i.e., a quasi-exciton-type transition), it is reasonable to assume that its unrelaxed excited state be positioned near the minimum of the conduction band. Based on these arguments we did the energy level diagram for both *F* centers and OH$_S^-$ defects for the five alkali hosts used (see Fig. 18). It is interesting to note that the observed energy separation between the relaxed excited state of the OH$_S^-$ ion and the unrelaxed ground state ($\sim 1s$) of *F* centers decreases for the KCl→RbI host change. For KI and RbI hosts a coincidence is observed of these energy positions thus supporting the assumption that, for these hosts, the OH^0 molecule leaves the vacancy giving rise to the *F* center formation. Establishing the experimental evidences for the *F* center formation during the OH$^-$ photodissociation process, it is necessary to have a more complete diagram to conciliate the phenomenology observed in this process, i.e., the fact that for temperatures around 50 K the molecule dissociates into hydrogen and oxygen defects besides showing fluorescence. A coordinate configurational diagram involving both *F* centers and OH$_S^-$ ions would be appropriate to phenomenologically describe this process.

Figure 19 shows a schematic diagram to illustrate all the processes following a UV(OH$^-$) excitation. At left is repre-

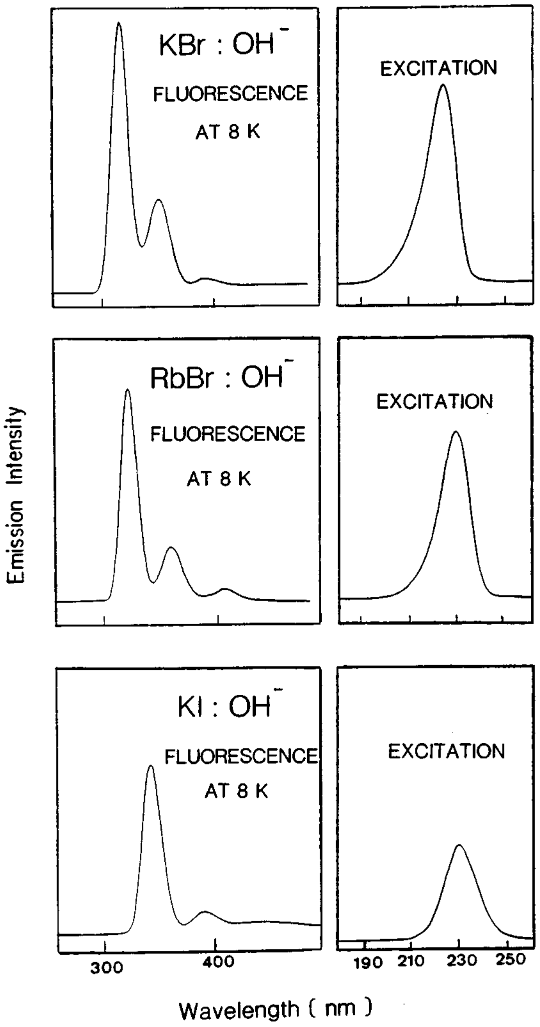

FIG. 15. Fluorescence and excitation spectra of substitutional OH^- defects measured at 8 K for several hosts containing 1×10^{17} OH^-/cm^3.

sented the total energy of $OH_S{}^-$ ions as a function of the Q_0, which is the coordinate of the local mode coupled to the vibronic states of the OH^- ions. In a perpendicular plane is described a parabola representing the total energy of the unrelaxed ground state of the F center as a function of the Q_F coordinate. A crossing point between these two systems is obvious. After a vertical OH^- excitation at the coordinate value Q_0, the molecule can reach the dissociative state having a very small chance to decay into H^0 and O^- ions. As the system remains briefly around this point ($\sim10^{-12}$ sec) it efficiently decays to the minimum of the parabola (A). During this relaxation to A, the system can cross over to the F center ground state (mechanism II) reaching point B. In this case, the F center and OH^0 interstitial molecule are formed. The position densities of both independent vibrational oscillators, observed at any instant, have a very small probability of overlapping at the crossing of the OH^- excited and F ground states. By increasing the temperature (50→77 K) the thermal population near the crossing point increases, making it more probable for the system to go through mechanism II. Of course, the available interstitial space to accommodate the OH^0 molecule also plays a decisive role for the mechanism (II). The estimated volume of the OH^0 molecule in its ($X^2\Pi_i$) ground state is 19.8 Å^3.[32] So, the host must have an available interstitial space larger than (19.8 Å^3) to allow the F center formation during the OH^- deexcitation process. The interstitial spaces (V_i) for all the studied hosts are listed in Table II.

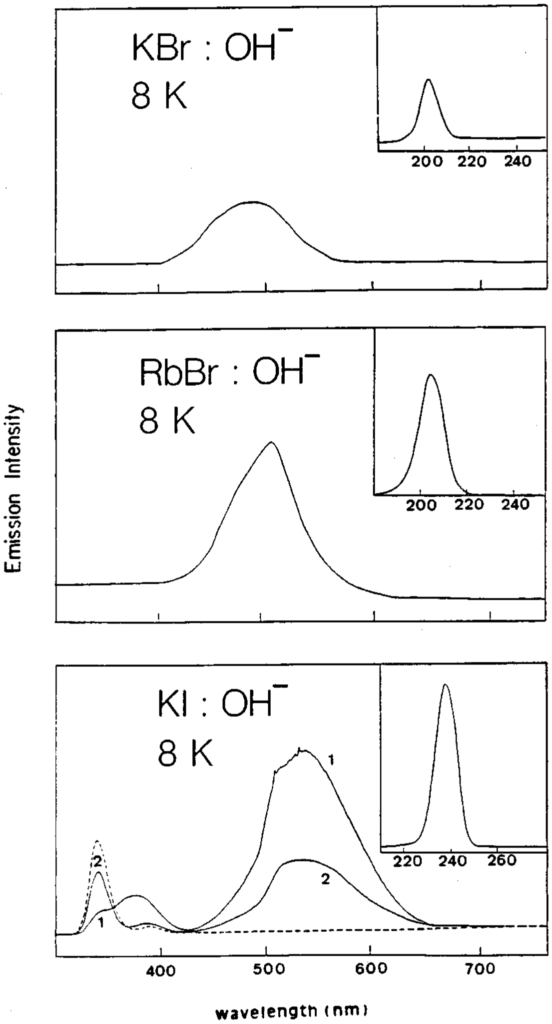

FIG. 16. Fluorescence spectra (measured at 8 K) of OH^- photodissociated KBr, RbBr, and KI crystals. The insets show the respective excitation spectra. The large emission bands in the range from 450 to 650 nm are due to α centers. In particular, for KI (curve 1) a new emission band is seen at 361 nm which was attributed to OH^- interstitial ions produced together with α centers by the second photodissociation channel of OH^- defects. Curve 2 shows the KI:OH^- spectrum after $T=240$ K. Broken line represents the initial fluorescence spectra of substitutional OH^- defects in KI crystal.

V. CONCLUSIONS

In this paper is presented a discussion of the electronic processes induced in alkali-halide crystals with the $OH_S{}^-$ defects in their excited state. The comprehensive study on the OH^- photodissociation done for several alkali-halide hosts showed that efficient electron traps can be produced after the $OH_S{}^-$ defects dissociation which can trap the con-

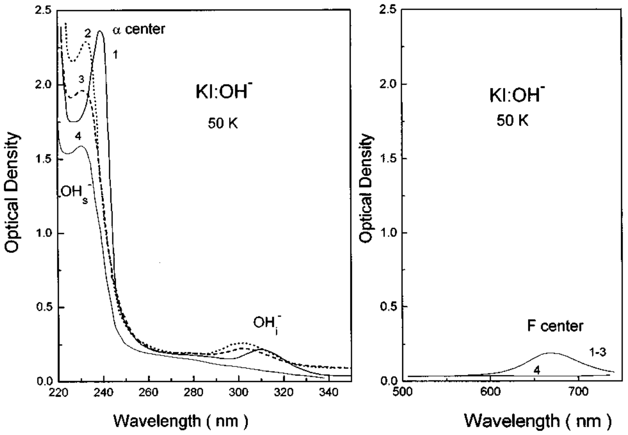

FIG. 17. Thermal effects on the new band at 312 nm in KI:OH$^-$. (1) Initial spectra measured at 50 K showing the α band (238 nm) and the 312-nm band, (2) after $T=240$ K, the α band (238→231) nm is seen and the new band (312→303) nm shifts; (3) after $T=300$ K; (4) spectrum exhibiting the OH$^-$ absorption band present in the host before the OH$^-$ photodissociation.

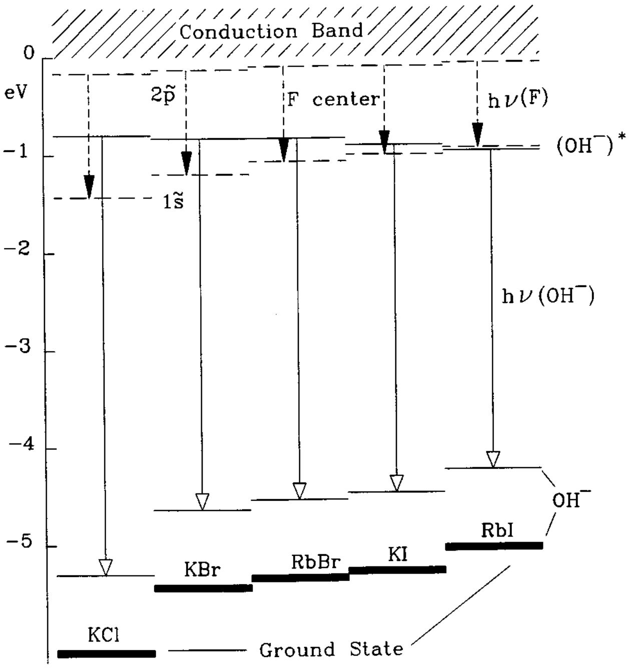

FIG. 18. Schematic energy level diagram for F centers and OH$^-$ substitutional defects for five alkali hosts. Dashed lines are used for representing the unrelaxed ground ($\sim1s$) and excited ($\sim2p$) states for F centers. Solid lines were used for representing the relaxed and unrelaxed ground and excited states for OH$^-$ substitutional defects. Dashed arrows were used to illustrate the emission transition for F centers while solid arrows were used for OH$^-$ ions. One must note that the energy separation between the relaxed excited state of the OH$_S{}^-$ ion and the unrelaxed ground state ($\sim1s$) of F centers decreases for KCl→RbI host change. For KI and RbI a coincidence is observed of these energy positions thus propitiating the F center formation during the UV excitation of OH$^-$ defects.

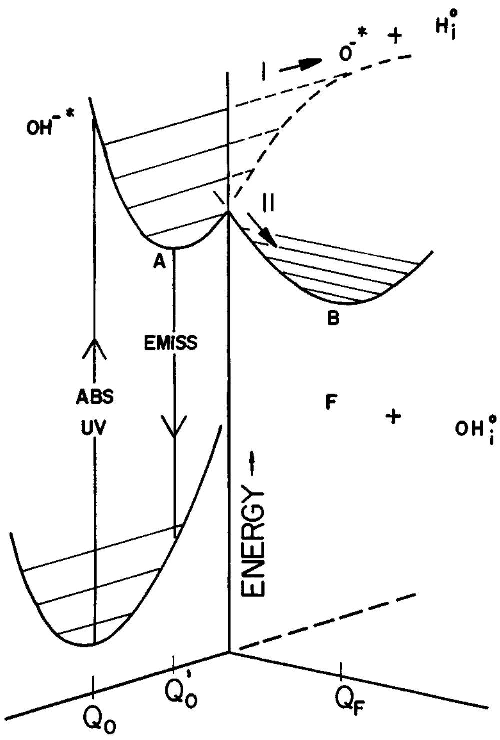

FIG. 19. Schematic coordinate configurational diagram involving both the F centers and the OH$_S^-$ defects. (I) indicates the dissociative process followed the UV OH$^-$ excitation. (II) indicates the new mechanism producing F centers and the OH$_i^0$ molecule due to the crossover point existence in KI and RbI hosts.

duction electrons produced in the high-energy irradiation. These ‘‘free’’ electrons are mainly produced by the radiation damage in the anionic sublattice. Two types of electron traps can be produced by the OH$^-$ dissociation: (a) deep traps, like the α center and OH$_i^0$ (interstitial molecules); (b) shallow traps, like the F centers producing metastable states. The deep traps (a) were observed in KI, RbI, and RbBr where the OH$^-$ direct photodissociates into an F center and OH$_i{}^0$ molecule at $T\approx77$ K. In that case, the creation of α centers is also observed at the expense of some F centers bleaching during the irradiation process. Anionic vacancies (α centers) also can be produced by the optical bleaching of O$_S{}^-$ centers in KCl, KBr, and RbCl (as was verified in KBr under hard UV irradiation). Anionic vacancies, as much as OH^0 interstitial molecules, can contribute to the formation of ionized color centers like F_2^+ centers. This fact has been observed for the F_2^+ center formation in OH$^-$-doped KCl and LiF under

TABLE II. The estimated volume of the interstitial space for all the studied hosts and the observation of the new deexcitation mechanism (II). NO represents not observed, $V=19.8$ Å^3 for the OH^0 ($X^2\Pi_i$) molecule (Ref. 32).

Host	V_i (Å^3)	Deexcitation mechanism (II)
KCl	14.6	NO
RbCl	16.8	NO
KBr	16.8	NO
RbBr	19.4	NO
KI	20.4	Yes
RbI	23.5	Yes

high-energy electron irradiation.[11,33] On the other hand, the shallow traps (F centers) also produced in KI and RbI for UV(OH^-) irradiation at $T \approx 77$ K work like temporary electron traps forming unstable F' centers (F center with two electrons). This situation is favorable to form neutral aggregate color centers as F_2 and F_3 centers. The main conclusion of this work is that OH_S^- defects, when present in the lattice of an alkali halide, have a strong tendency to decrease the formation of aggregate color centers with an excess of electrons such as F_2^- centers by the radiation damage process.

---

[*] Electronic address: lgomes@net.ipen.br

[1] J. F. Pinto, E. Efstratios, and C. R. Pollock, Opt. Lett. **11**, 519 (1986).
[2] D. Wandt, W. Gellermann, F. Luty, and H. Welling, J. Appl. Phys. **61**, 864 (1987).
[3] E. Georgiou, J. F. Pinto, and C. R. Pollock, Phys. Rev. B **35**, 7636 (1987).
[4] F. Fischer, H. Grundig, and R. Hilsch, Z. Phys. **189**, 79 (1966).
[5] P. Hennel, Phys. Status Solidi A **46**, 147 (1978).
[6] D. Wandt and W. Gellermann, Opt. Commun. **61**, 405 (1987).
[7] L. Gomes and F. Luty, Phys. Rev. B **30**, 7194 (1984).
[8] W. Gellermann, F. Luty, K. Koch, and G. Litfin, Phys. Status Solidi A **57**, 411 (1980).
[9] W. Gellermann, F. Luty, K. Koch, and H. Welling, Opt. Commun. **35**, 430 (1980).
[10] W. Gellermann and F. Luty (unpublished).
[11] W. Gellermann, J. Phys. Chem. Solids **52**, 249 (1991).
[12] L. C. Courrol and L. Gomes, J. Phys. Chem. Solids (to be published).
[13] F. Kerkoff, Z. Phys. **158**, 595 (1960).
[14] L. Gomes and S. P. Morato, Radiat. Eff. **73**, 139 (1983).
[15] C. J. Delbecq, B. Smaller, and P. H. Yuster, Phys. Rev. **104**, 599 (1956).
[16] H. Hartel and F. Luty, Phys. Status Solidi **12**, 347 (1965).
[17] G. Schaefer, J. Phys. Chem. Solids **12**, 233 (1960).
[18] B. Fritz, J. Phys. Chem. Solids **23**, 375 (1962).
[19] S. P. Morato, L. C. Courrol, L. Gomes, V. Kalinov, and A. Schadarevich, Phys. Status Solidi B **163**, K61 (1990).
[20] I. M. Ranieri *et al.*, J. Cryst. Growth **166**, 423 (1996).
[21] L. C. Courrol, L. Gomes, and S. P. Morato, Phys. Rev. B **51**, 3344 (1995).
[22] M. B. Camargo, L. Gomes, and S. P. Morato, Opt. Mater. **4**, 597 (1995).
[23] L. Gomes and F. Luty, Phys. Rev. B **52**, 7094 (1995).
[24] V. Dierolf and F. Luty, Solid State Commun. **98**, 513 (1996).
[25] H. Kostlin, Solid State Commun. **3**, 81 (1965).
[26] J. Rolfe, Phys. Rev. Lett. **1**, 56 (1958).
[27] J. A. Cape, Phys. Rev. **122**, 18 (1968).
[28] S. P. Morato and F. Luty, Phys. Rev. B **22**, 4980 (1980); S. P. Morato, Ph.D. thesis, University of Utah, 1975.
[29] S. P. Morato and L. Gomes, Solid State Commun. **41**, 653 (1982).
[30] S. P. Morato and F. Luty, J. Phys. C **6**, 155 (1980).
[31] A. G. Badalyan and P. G. Baranov, Sov. Phys. Solid State **22**, 2020 (1980).
[32] P. A. Cade, F. W. Bader, and J. Pelletier, J. Chem. Phys. **54**, 3517 (1971).
[33] L. C. Courrol, L. Gomes, and I. M. Ranieri, Phys. Rev. B **42**, 4741 (1990).